PERGAMON

International Journal of Heat and Mass Transfer 43 (2000) 3481–3496

International Journal of HEAT and MASS TRANSFER

www.elsevier.com/locate/ijhmt

Diffusion within a porous medium with randomly distributed heat sinks

Vladimir V. Kulish, José L. Lage*

Mechanical Engineering Department, Southern Methodist University, PO Box 750337 Dallas, TX 75275-0337, USA

Abstract

Heat sinks filled with phase-change material, a design concept suitable for the thermal management of electronic airborne systems, find limited applicability at present due to lack of structural rigidity and poor isothermal cooling characteristics. A composite heat sink device (CHSD) is a new design concept proposed in this work, which combines the thermal benefit of the phase-change material with the structural rigidity provided by a solid porous matrix. The device consists of a solid porous matrix with pores filled with capsules containing a phase-change material. Numerical simulations of a CHSD steady-model indicate the existence of a maximum capsule density beyond which a transition from *disperse* diffusion (when all capsules actively participate in the diffusion process) to *concentrate* diffusion (when the capsules close to the heated surface shield the capsules placed further away) occurs. This observation is important for optimizing the volume of the CHSD.

1. Introduction

Current trends in electronic packaging for aerospace applications indicate that the electric power dissipation flux of these devices will surpass 100 W/cm^2 by the end of the century [1]. Innovative cooling techniques are fundamental to managing this increased dissipating power along with stiff temperature requirements and further miniaturization. Extraordinary heat transfer rates, in excess of 200 W/cm^2, have already been attained by advanced microchannel heat exchangers under convective boiling heat transfer [2].

Similar to microchannel heat sinks, microporous [3,4] heat sinks improve the weak heat transfer at the fluid side of solid–fluid heat exchangers by increasing the interface area (fin effect) with the advantage of inducing fluid mixing (dispersion and turbulence effects) within convective cooled devices. A thorough review of heat transfer enhancing techniques was offered recently by Webb [5].

Out of all the liquid-based devices, only the boiling-based device does not induce a large temperature variation when cooling extended surfaces. However, boiling devices tend to require several components, including fluid storage, and a flow loop that occupies a large volume.

A solid-to-liquid phase-change heat sink is another alternative when isothermal cooling is important, as in the thermal management of microelectronics [6]. Moreover, when considering systems designed under stringent volume constraints a solid-to-liquid phase change device is more advantageous than boiling devices for not requiring a flow loop,

* Corresponding author. Tel.: +1-214-768-2631; fax: +1-214-768-4173.

E-mail address: jll@seas.smu.edu (J.L. Lage).

0017-9310/00/$ - see front matter
PII: S0017-9310(99)00385-3

Nomenclature

A	surface area	λ	curve fitting parameter $= \rho^{-1/3}$
c	specific heat	τ	curve fitting parameter $= 1 + \rho$
d	representative linear dimension	ρ	capsule density $= V_e/V$
j	nodes	θ	nondimensional temperature $= (\langle T\rangle - T_e)/(T_0 - T_e)$
k	thermal conductivity (W/m K)	ω	weight-parameter for S.O.R. scheme
L	characteristic length		
N	number of grid sites		
$\mathbf{n}$	unit vector	*Subscripts*	
$\mathbf{q}''$	heat flux vector (W/m^2)	b	boundary
t	time	e	PCM saturation temperature
T	temperature	eff	effective
$\langle T\rangle$	volume average temperature	i	component
U	overall heat transfer coefficient (W/m^2 K)	s	structural material
V	volume	r	representative
δ	pseudo-conductivity (W/m K)	t	transfer material

even though they do require to be *recharged* — solidified — for continuous (cyclic) use. The smaller density variation from solid to liquid, as compared to the density variation from liquid to gas found in boiling devices, is also an important advantage in terms of the total volume necessary for the system.

Therefore, solid-to-liquid phase-change heat sinks are ideally suited for electronic airborne systems, including those used in satellites, because of their reduced volume, isothermal cooling characteristic, and mechanical simplicity (reliability).

The simplest solid-to-liquid phase-change heat sink design is that of a homogeneous phase-change material, filling an enclosure. As an isothermal heat sink, the thermal capacity of the device is proportional to the volume and latent heat of the PCM. Hence, for a chosen PCM, the isothermal cooling capacity of the device increases with the PCM volume. In practice, the isothermal cooling characteristic of a simple solid-to-liquid phase-change heat sink deteriorates very rapidly as the solid material liquefies near the heated surface(s). This is so because of the temperature gradient that develops within the liquid phase of the PCM (for driving the heat flux from the heated surface to the liquid/solid interface). Moreover, the density variation from solid to liquid, although small, imposes mechanical stresses on the enclosure, compromising the structural integrity of the device.

An alternative to a homogeneous solid-to-liquid phase-change heat sink consists of filling the pores of an enclosed solid porous matrix with a PCM [7]. The solid porous matrix provides superior structural rigidity to the device, it hinders the convection within the liquid region, and, if made of a good thermal conductor, it enhances the heat transfer from the heated surface to the solid–liquid interface, reducing the temperature gradient within the liquid region (similar to having fins within the PCM region, [8]).

We consider a more complex system in which the phase-change material filling the pores of the solid matrix is encapsulated and not continuous. The objectives of this modification are to (1) minimize the stresses on the system following the expansion/contraction of the phase-change material, (2) reduce void formation during the solidification and shrinkage of the phase-change material, and (3) enhance thermal performance of the device by increasing the surface area of the phase-change material and by suppressing even more the natural convection within the liquefied region (now contained within small capsules).

A practical difficulty in building a heat sink device with encapsulated phase-change material is to distribute the capsules within the pores of the solid matrix. One solution being considered is to inject through the pores of the solid matrix a liquid solution (transfer material, or carrier) containing the capsules with phase-change material. Upon solidification of the transfer material, the device would become a *composite heat sink device* (CHSD) consisting of three main constituents: the solid porous matrix, the transfer material in the solid phase, and the encapsulated phase-change material.

During operation, only the phase-change material inside the capsules is to melt (or solidify, during recharging). The transfer material is chosen such as to present a melting temperature above the operational temperature of the CHSD, i.e., the transfer

material remains solid during operation (the transfer material is liquefied only when used for injecting the encapsulated PCM into the porous matrix). Therefore, there is no possibility of segregation of the encapsulated material as the PCM-filled capsules will lie in solid media (i.e., the solidified transfer material) throughout the operation of the device.

Obviously, several issues have to be considered for the practical implementation of the CHSD, such as a porous matrix, the carrier material, and encapsulated PCM thermal and mechanical properties. Another important issue, considered here, is the amount (density) of encapsulated PCM placed inside the pores of the solid matrix, and how it affects the heat transfer process.

The density of encapsulated PCM within the device (defined as the volume of PCM per total volume of the device) is an important design parameter. If the density is too high, the thermal behavior of the device will tend towards that of a simple solid-to-liquid phase-change (as the volume of the solid porous matrix and of the transfer material becomes negligible). If the density is too low, the latent thermal capacity of the device is reduced (because of the lack of PCM) compromising the latent cooling characteristic of the device. It is important then to quantify the effect of encapsulated PCM density on the thermal performance of a CHSD.

2. Theoretical model

Consider the main constituents of the CHSD as the solid matrix (s), the solidified transfer material (t), for injecting into the capsules, and the encapsulated phase-change material (e) (see Fig. 1(a)). Neglecting the convection within the capsules filled with PCM, the microscopic equation modeling the diffusion transport within each heat sink constituent with constant properties, can be written as:

$$\rho c \frac{\partial T}{\partial t} = -\nabla \cdot \mathbf{q}'' \tag{1}$$

where ρ and c are the density and specific heat of the

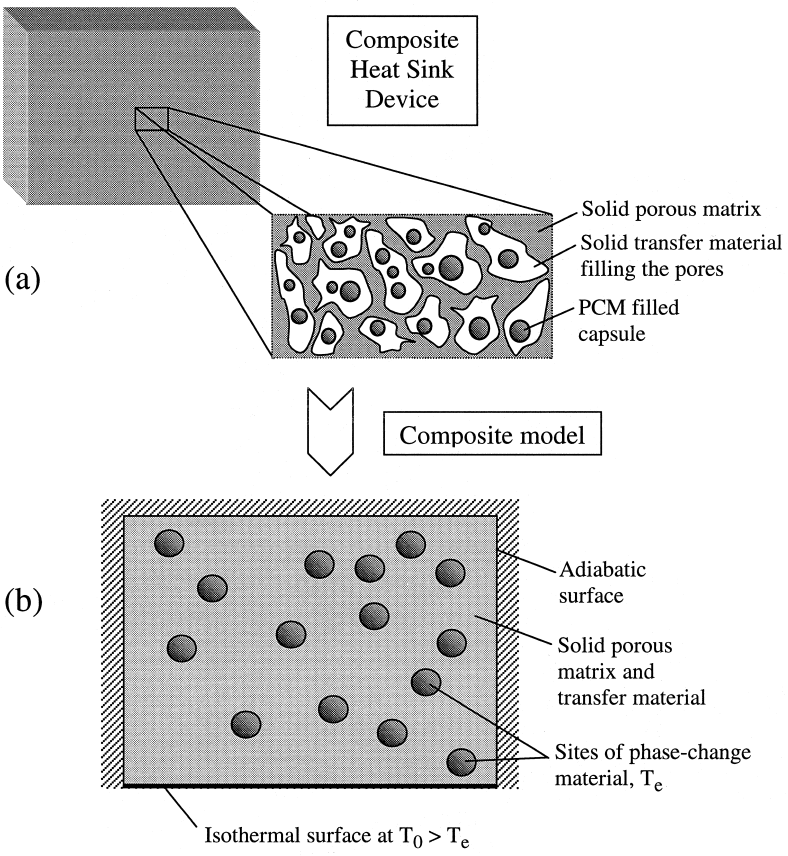

Fig. 1. (a) Sketch of the composite heat sink device showing detail of the internal structure; (b) composite model: solid porous matrix and transfer material bounded by external surfaces and internal surfaces delimiting regions occupied by capsules with PCM.

constituent, T is the local temperature, and $\mathbf{q}''$ is the heat flux, related to the local temperature gradient via Fourier's law,

$$\mathbf{q}'' = -k\nabla T \tag{2}$$

where k is the (molecular) thermal conductivity of the constituent (assumed uniform).

To focus attention on the heat transfer process during phase-change, the encapsulated PCM is considered to be maintained at the saturation temperature T_e. In this case, one does not need to solve the heat transport inside the capsules, because the capsules will be isothermal throughout the phase-change process (obviously, if in practice the latent cooling capacity of the heat sink is surpassed then the temperature of the capsules will change; this sensible heating process is of no interest to the present work). It is possible then to consider a simpler two-constituent model of the heat sink with only the solid porous matrix and the transfer material. For the region occupied by the solid porous material, s-region, one has

$$(\rho c)_s \frac{\partial T_s}{\partial t} = k_s \nabla^2 T_s \tag{3}$$

where T_s, $(\rho c)_s$, and k_s are the local temperature, thermal capacity, and conductivity of the solid matrix, respectively. This equation can be solved with appropriate boundary conditions. One of the boundary conditions, i.e. isothermal, isoflux, adiabatic, or a combination of them, is set along the heated surface area A_0 of the heat sink in contact with the solid material. The other boundary condition imposed along the interface area A_{st} between the solid matrix and the transfer material, is $T_s = T_t$, where T_t is the transfer material local temperature. For the solid transfer material region, t-region, one has:

$$(\rho c)_t \frac{\partial T_t}{\partial t} = k_t \nabla^2 T_t \tag{4}$$

where $(\rho c)_t$ and k_t are the thermal capacity and conductivity of the thermal material, respectively. One boundary condition in this case is $\mathbf{n}_{st} k_t \nabla T_t = \mathbf{n}_{st} k_s \nabla T_s$, representing a balance of heat flux across the solid matrix interface with the transfer material. The interface has surface area A_{st} and normal unit vector $\mathbf{n}_{st}$. The second and final boundary condition, $T_t = T_e$, is set along the interface of the transfer material with the encapsulated PCM, with surface area A_{te} (recall that only the phase-change process is being considered, during which the PCM temperature remains constant and equals T_e).

Eqs. (3) and (4) can be used to simulate the transient diffusion process within the heat sink during phase-change. The difficulty is the need to describe (locate) precisely the region occupied by each constituent and the related interfaces. To circumvent this difficulty, we consider a model that, at least approximately, predicts the diffusion process inside the composite heat sink.

The model allocates discrete regions within the device for the capsules of PCM, as shown in Fig. 1(b). The remaining volume is then occupied by the solid porous matrix and the solid transfer material. Consider a certain volume V_r of the remaining volume with representative dimension d, where d is much smaller than L (the characteristic dimension of the heat sink), much larger than d_s (the characteristic dimension of the solid matrix) and d_t (the characteristic dimension of the transfer material). Keep in mind that the capsules filled with PCM are not included within V_r.

As defined, V_r is a *representative elementary volume* (REV). Our model is developed by applying the method of volume averaging [9] to transform the effects of the internal geometry of the heat sink from a microscopic level to a macroscopic representative elementary volume level (REV-level). For a two-component medium the derivation is similar to that for a fluid saturated porous medium shown in [10]. The resulting equation is

$$(\rho c)_{eff} \frac{\partial \langle T \rangle}{\partial t} = k_{eff} \nabla^2 \langle T \rangle \tag{5}$$

where $\langle T \rangle$ is the representative volume averaged temperature within V_r, and $(\rho c)_{eff}$ and k_{eff} are respectively the effective thermal capacity and conductivity of the REV, formally defined as

$$(\rho c)_{eff} = \left[\frac{V_s}{V_r} (\rho c)_s + \frac{V_t}{V_r} (\rho c)_t \right] \tag{6}$$

$$k_{eff} = \left(\frac{V_s}{V_r} k_s + \frac{V_t}{V_r} k_t \right) + \frac{(k_s - k_t)}{V_r} \int_{A_{st}} \mathbf{n}_{st} \cdot \delta_s \, dA \tag{7}$$

where V_s and V_t are the volumes occupied by the solid matrix and by the transfer material, respectively, within V_r, and δ_s is a pseudo-conductivity parameter (a tensor, in general). (Note: the derivation of Eq. (5) assumes thermal equilibrium between the solid porous structure and the transfer material, i.e., $\langle T \rangle = \langle T \rangle_s = \langle T \rangle_t$. This is a reasonable assumption as long as the two components have similar thermal conductivities.)

These effective parameters are lumped parameters, at the REV level, that characterize the transport process within the REV without the need to describe the internal geometry of the REV. The problem is then transferred from modeling the heat diffusion process per se to determining the effective conductivity of the medium as a function of the structural and physical (molecular) properties of each constituent existing within the REV. Observe that once k_{eff} is known, Eq.

(5) is easily solved by applying a suitable initial condition and boundary conditions (in terms of $\langle T\rangle$). It is, unfortunately, extremely difficult to resolve the integral of Eq. (7).

Alternatively, one can combine the effective heat sink diffusivity, defined in Eq. (7), with the heat sink overall heat transfer coefficient U of the CHSD during the phase-change process, defined as

$$U = \frac{\mathbf{q}''}{(T_0 - T_e)} \tag{8}$$

where $\mathbf{q}''$ is the heat flux crossing the heated boundary of the heat sink and T_0 is the boundary temperature. Notice that at the steady-state U is constant.

Observe that all quantities to the right of the equal sign in Eq. (8) are easily obtained in the laboratory. Eliminating $\mathbf{q}''$ from Eq. (8) using Eq. (2) written as $\mathbf{q}'' = k_{\text{eff}}|\nabla\langle T\rangle|$, where $|\nabla\langle T\rangle|$ is the temperature gradient at the boundary of the heat sink, one obtains,

$$k_{\text{eff}} = U\left(\frac{1}{|\nabla\theta|}\right) \tag{9}$$

where $|\nabla\theta|$ is the surface gradient of the nondimensional temperature, defined as $\theta = (\langle T\rangle - T_e)/(T_0 - T_e)$, at the boundary of the heat sink. Observe that $|\nabla\theta|$ represents the characteristic diffusion length of the domain, in m^{-1}.

If one can obtain $|\nabla\theta|$ independently of k_{eff}, then one can find k_{eff} from Eq. (9). Indeed, the term $|\nabla\theta|$ can be determined independently of k_{eff} by solving the steady-state version of Eq. (5). In this case Eq. (5) reduces to the Laplace equation in $\langle T\rangle$ independent of k_{eff}. This detail is explored in the next section discussing the numerical simulation of the steady diffusion process in the composite heat sink device.

3. Numerical simulations

We consider now the use of the steady-state version of Eq. (5), namely $\nabla^2\langle T\rangle = 0$, to simulate the diffusion within the composite heat sink. For simplicity, the domain of interest is chosen as a cube of side unity. The bottom face of the cube is assumed to be isothermally heated, maintained at $\langle T\rangle = T_0 > T_e$ (or $\theta = 1$), with all others faces assumed adiabatic with $\partial\langle T\rangle/\partial n = 0$ (or $\partial\theta/\partial n = 0$), where n is the coordinate with a direction perpendicular to the adiabatic face (see Fig. 1(b)).

The capsules distributed within the heat sink are simulated by selecting a random (normal) distribution of sites (nodes) within the numerical domain and setting the temperature value at these sites equal to T_e, or in nondimensional form, $\theta = \theta_e = 0$.

The only parameter controlling the phase-change site distribution is the capsule density, $\rho = V_e/V$, where V_e is the total volume occupied by the capsules and V is the total volume of the domain. This parameter represents the relative volume, within the cube, occupied by the encapsulated phase-change material.

For a given density value, $0 \le \rho \le 1$, the number of capsule sites inside the domain is calculated as $N_e = \rho N$, where N is the total number of available sites (grid nodes inside the domain). Observe that the nodes along the surfaces (boundary) of the cube are unavailable for the phase-change material, and are therefore not counted on N.

The diffusion equation was discretized using central differences and solved using the S.O.R. technique with $\omega = 1.6$ which provides the minimum amount of iterations for convergence. Numerical convergence was determined when the maximum deviation, between consecutive iterations, of temperature values among all nodes becomes smaller than 0.01. A $25 \times 25 \times 25$ equally spaced orthogonal computational grid distributed within the cube was tested against a $50 \times 50 \times 50$ grid showing less than 0.1% maximum variation in the local temperature values for the same capsule density ρ.

For each value of ρ a volume averaged nondimensional temperature was computed as

$$\bar{\theta} = \frac{1}{N}\sum_j \theta_j \tag{10}$$

where θ_j is the temperature value at each node within the domain. Also calculated was the absolute value of the total surface temperature gradient,

$$|\nabla\theta| = \sum_b \frac{\partial\theta}{\partial n} \tag{11}$$

where the summation is done over all the heated boundary nodes. The surface temperature gradient of Eq. (11) is computed numerically via an algebraic approximation. This parameter is the one to be used in Eq. (9) for determining k_{eff}.

4. Results

The temperature distribution within the domain is seen in Fig. 2, for instance, where the $\theta = 0.10$ isosurface is plotted for capsule density varying from 0.5 to 10%. Notice that the capsule sites account for a very small number of available sites when the capsule density is small. The isosurface, limiting from below the region of the cube with temperatures smaller than 0.10, is irregular in this case.

Observe that some isolated isosurfaces can be seen

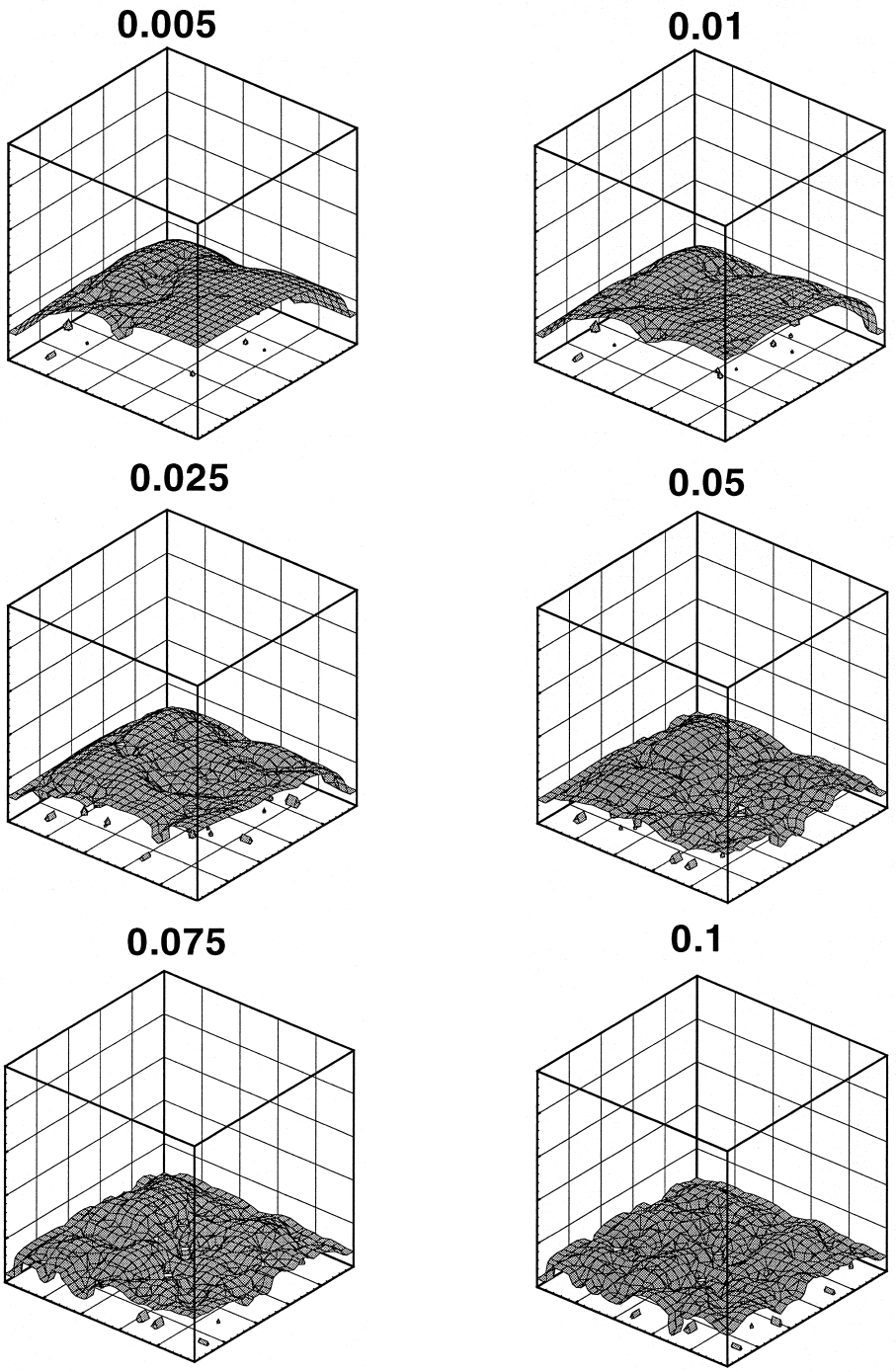

Fig. 2. Effect of capsule density ρ on the $\theta = 0.10$ isosurface distribution for $\rho \leq 0.1$; numbers on top of each cube reflect the capsule density of each case.

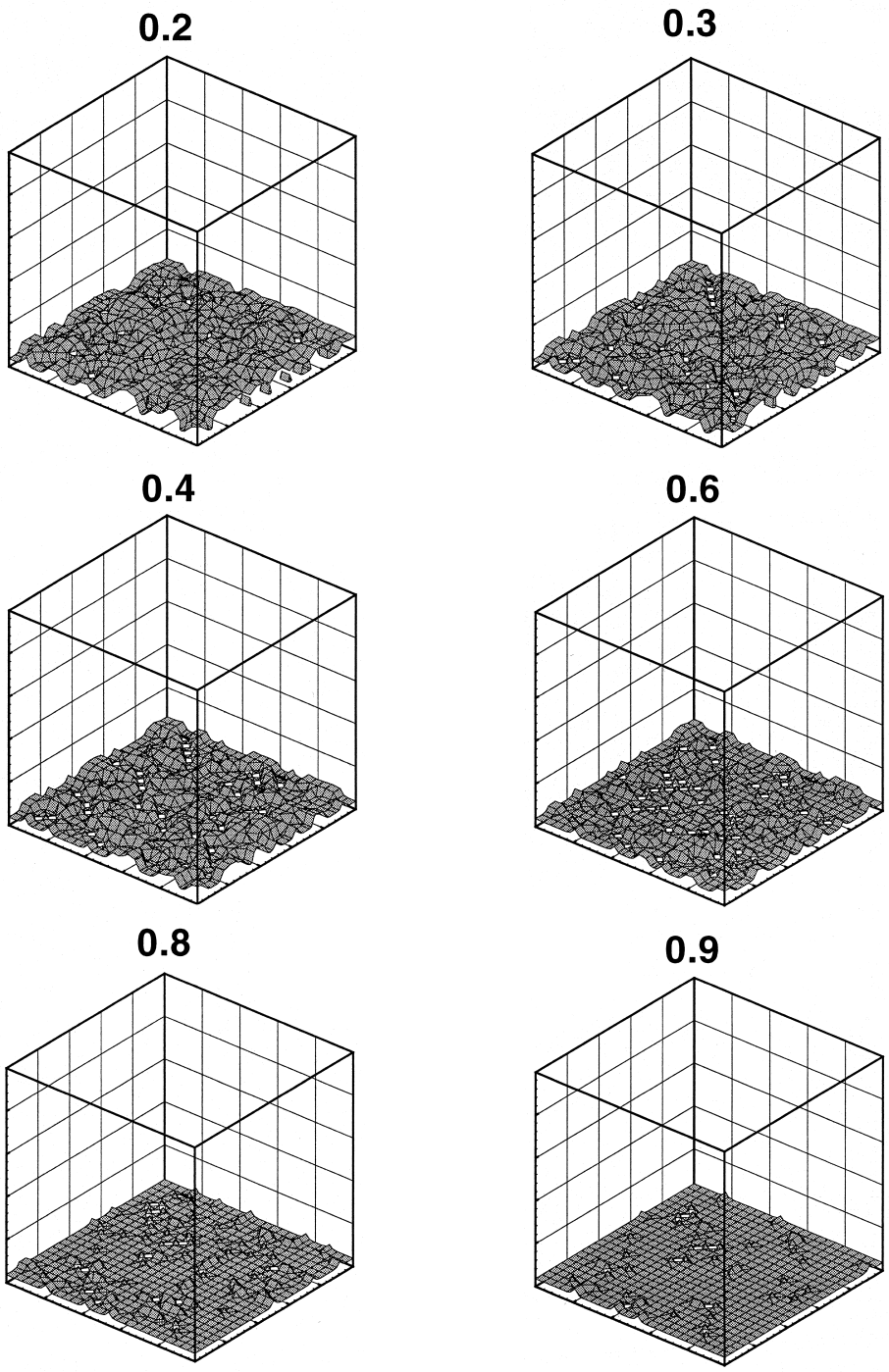

Fig. 3. Effect of capsule density ρ on the $\theta = 0.10$ isosurface distribution for $\rho \geq 0.2$; numbers on top of each cube reflect the capsule density of each case.

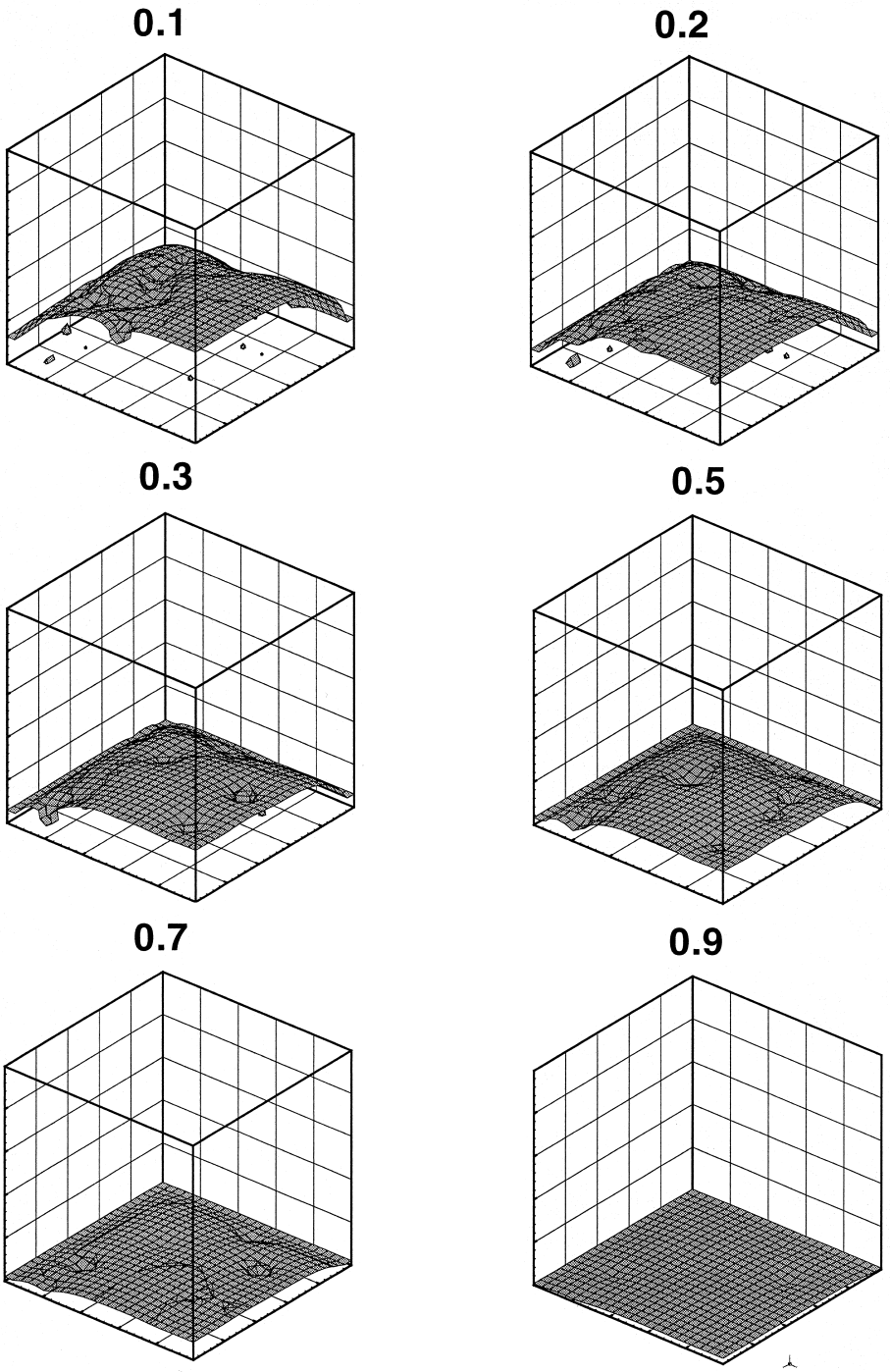

Fig. 4. Nondimensional temperature isosurface distribution for $\rho = 0.005$; numbers on top of each cube reflect the corresponding temperature isosurface value in each case.

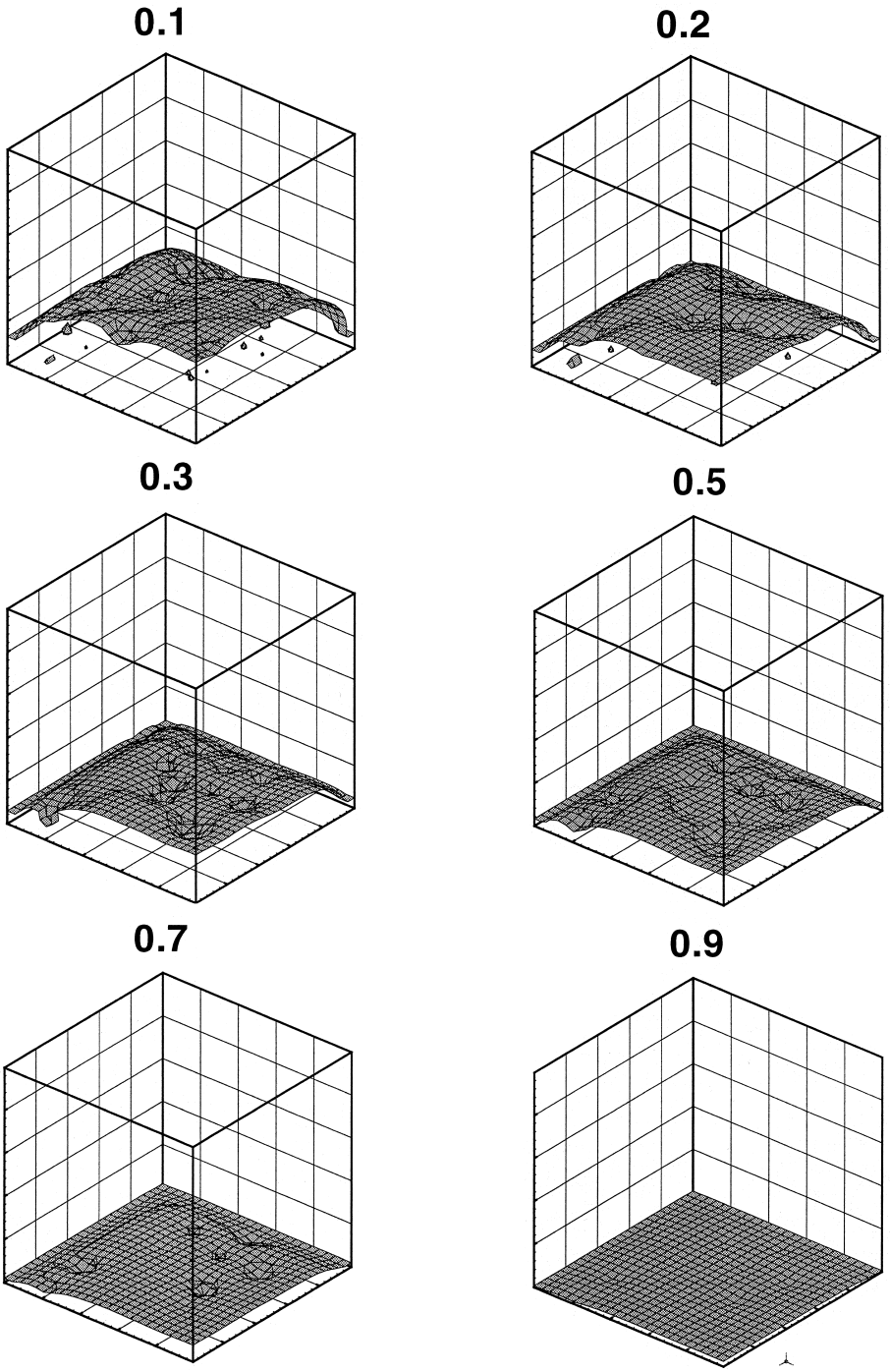

Fig. 5. Nondimensional temperature isosurface distribution for $\rho = 0.01$; numbers on top of each cube reflect the corresponding temperature isosurface value in each case.

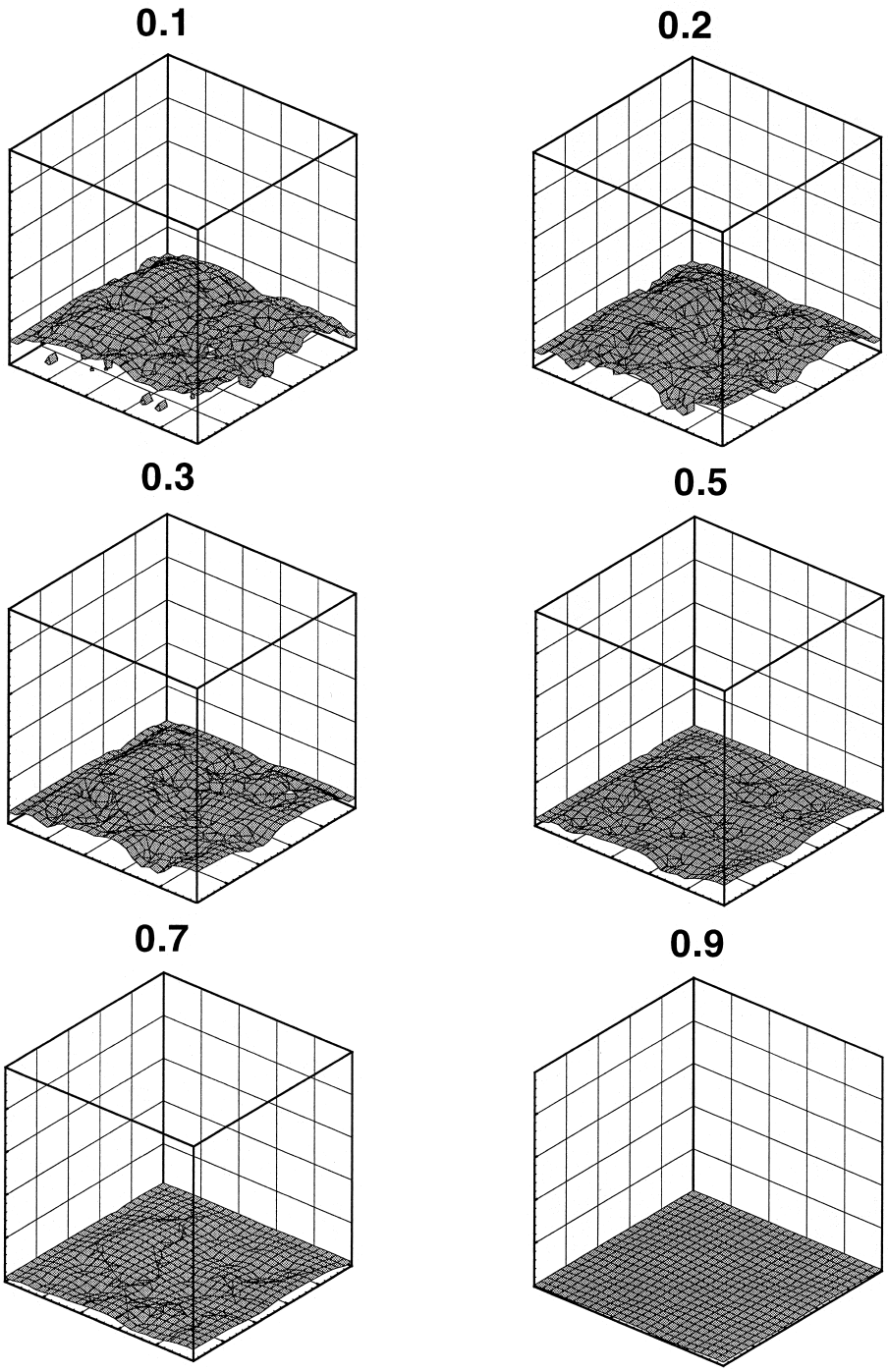

Fig. 6. Nondimensional temperature isosurface distribution for $\rho = 0.05$; numbers on top of each cube reflect the corresponding temperature isosurface value in each case.

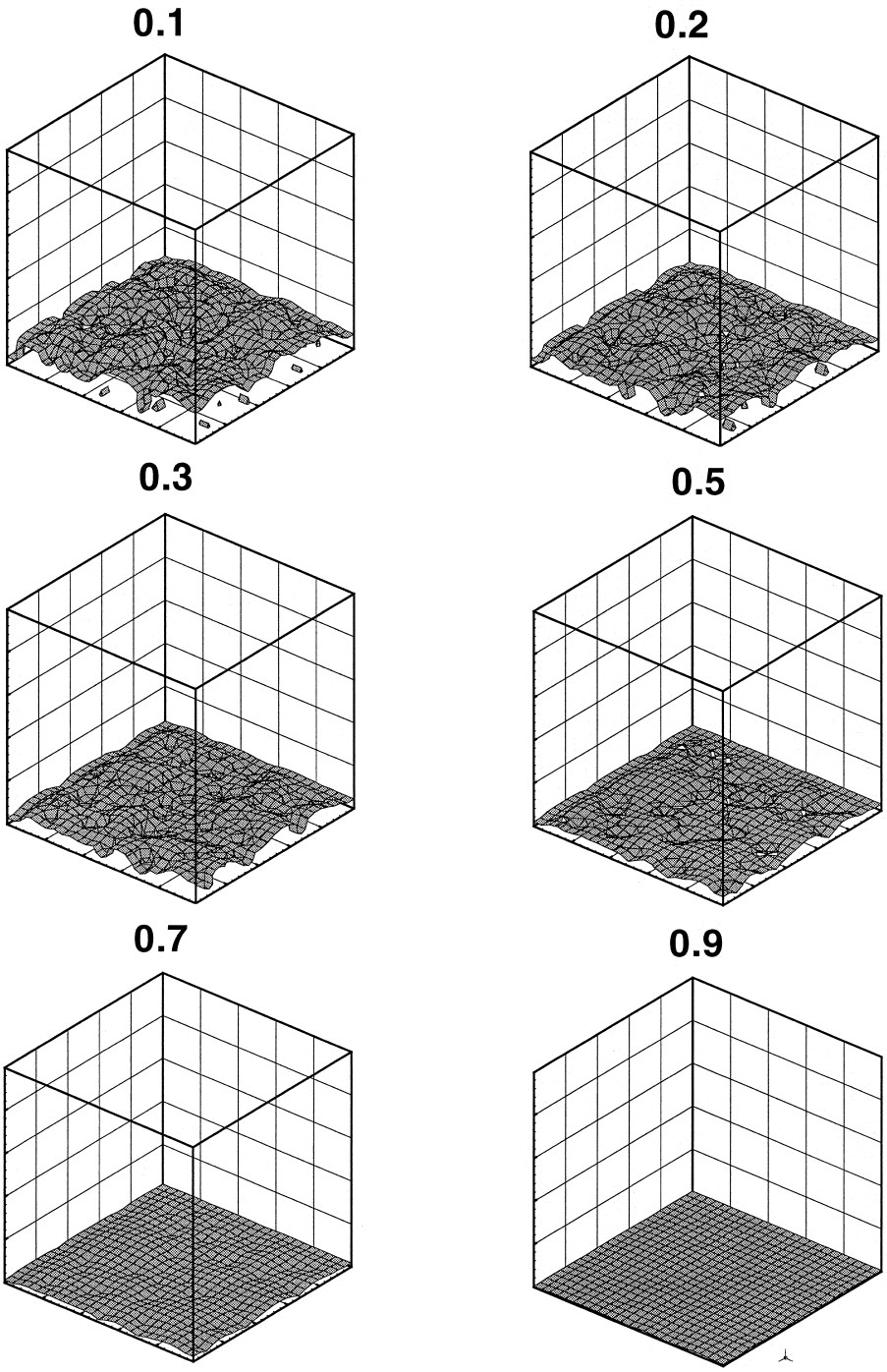

Fig. 7. Nondimensional temperature isosurface distribution for $\rho = 0.10$; numbers on top of each cube reflect the corresponding temperature isosurface value in each case.

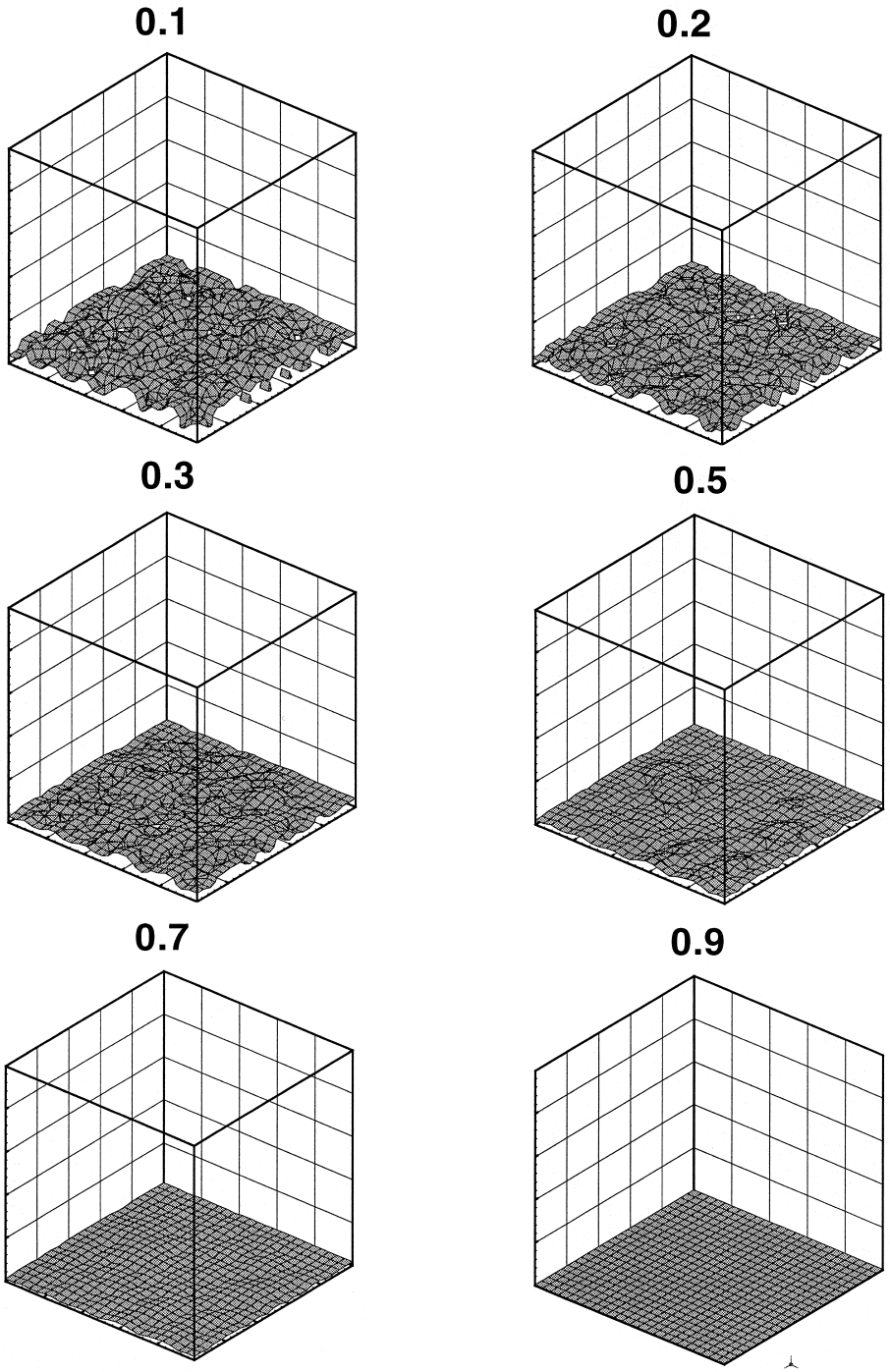

Fig. 8. Nondimensional temperature isosurface distribution for $\rho = 0.20$; numbers on top of each cube reflect the corresponding temperature isosurface value in each case.

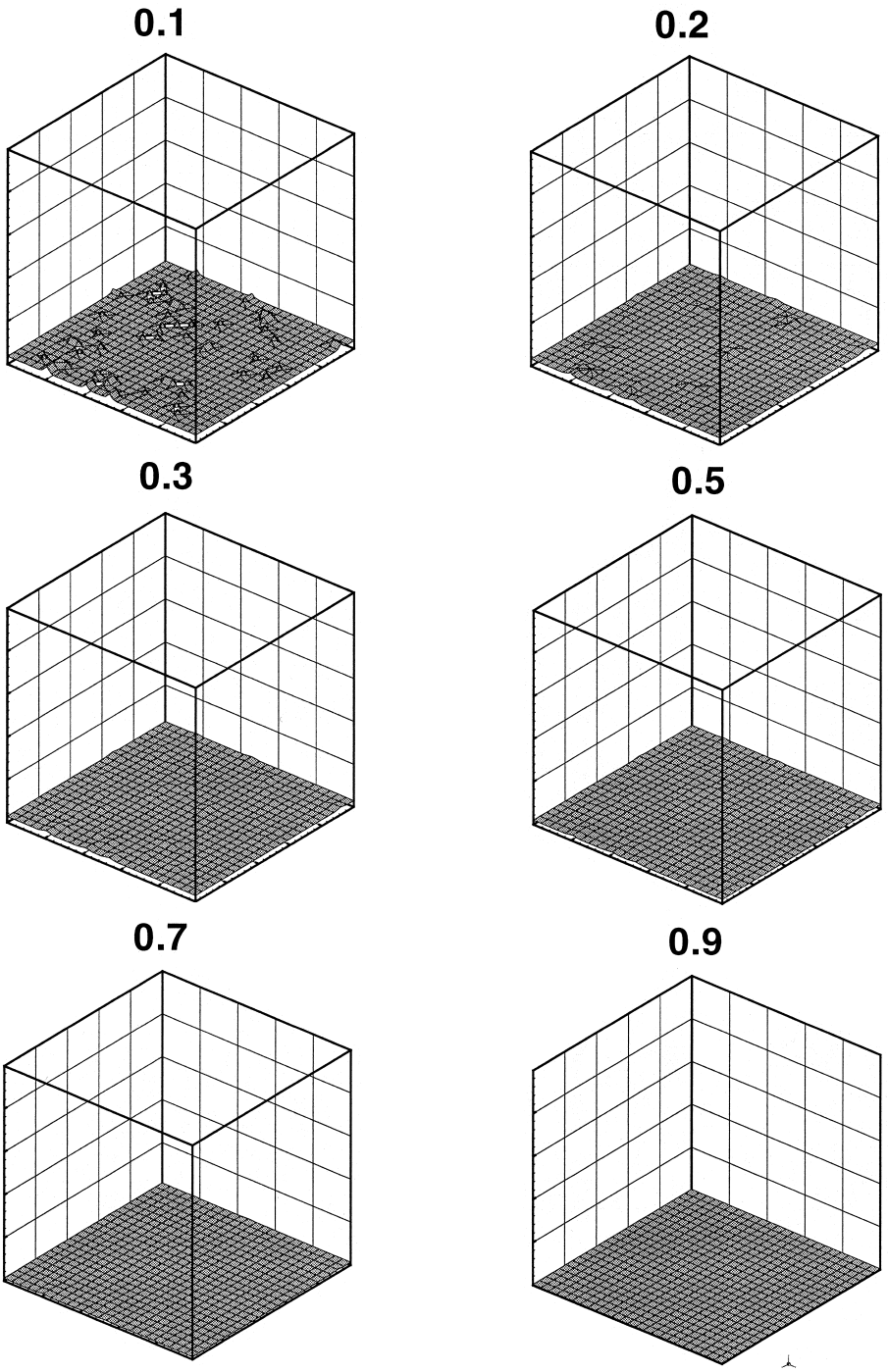

Fig. 9. Nondimensional temperature isosurface distribution for $\rho = 0.90$; numbers on top of each cube reflect the corresponding temperature isosurface value in each case.

around individual capsules in all plots of Fig. 2. As the capsule density increases, the number of sites occupied by the encapsulated PCM increases and the isosurface $\theta = 0.10$ moves relatively closer to the heated bottom face of the cube. This phenomenon reflects a shielding effect promoted by the capsules closer to the heated surface of the cube as the capsule density increases.

The sites, occupied by phase-change material placed far from the heated face of the cube, are increasingly shielded by the capsule sites near the heated face. This effect becomes more evident in Fig. 3 where results for capsule density greater than 20% are presented. Observe that the relative location of isosurface $\theta = 0.10$, relative to the bottom face, changes more pronouncedly as the capsule density increases from 0.5 to 10%. The location of the isosurface $\theta = 0.10$ varies much less from case to case when the capsule density is varied from 20 to 90%. Isosurfaces surrounding individual capsules can no longer be seen in the frames of Fig. 3. The main event observed in Fig. 3 is the progressive smoothing of the isosurface $\theta = 0.10$. As the capsule density increases, the isosurface $\theta = 0.10$ becomes increasingly closer and more parallel to the bottom (heated) face of the cube.

We can speculate then, that for capsule density between 10 and 20%, the diffusion process becomes increasingly dominated by the large number of capsules near the heated surface of the domain. Not much happens at the interior of the domain with the heat transfer having a small chance of reaching the capsules placed in there. Notice for density equal to 90% that the isosurface $\theta = 0.10$ is almost perfectly parallel to the heated surface of the domain.

Consider now Fig. 4 where several isosurfaces are plotted for the case of capsule density equal to 0.5%. The isosurfaces are relatively smooth indicating a large distance between capsules (dispersed distribution). Increase the capsule density to 1, 5 and 10% (see Figs. 5–7, respectively) and notice how the isosurfaces become rippled indicating the presence of more capsules close together competing for the heat coming from the bottom face of the cube. Observe also how the isosurfaces of same value continuously approach the bottom surface as the capsule density increases.

There is not much difference between the isosurfaces with $\theta > 0.50$ or capsule density equal to 20 and 90%, shown respectively in Figs. 8 and 9. This is in accord with the previous observation that for $\rho > 0.20$ the diffusion process is dominated by the capsules near the heated bottom face of the cube.

Fig. 10 presents the average temperature $\bar{\theta}$ vs. the capsule density ρ. The curve of Fig. 10 resembles the dimensionless velocity distribution of a boundary layer flow over a flat surface, with $\bar{\theta}$ playing the role of the fluid velocity and ρ playing the role of the distance from the surface. The temperature variation can be approximately represented by two functions: a *boundary layer* function (for small ρ) and a *mainstream* function far from the boundary (for large ρ). This observation allows the introduction of two equations (asymptotes) that fit quite well the numerical results, namely

$$\bar{\theta}(\rho) = 1 - e^{(-0.007\tau\lambda^{2+\rho})} \quad \text{for} \quad \rho < 0.16 \tag{12}$$

$$\bar{\theta}(\rho) = -0.007\lambda \ln(\rho) \quad \text{for} \quad \rho > 0.16 \tag{13}$$

where $\tau = 1 + \rho$, and $\lambda = (1/\rho)^{1/3}$. Observe that the average distance between capsule sites is proportional

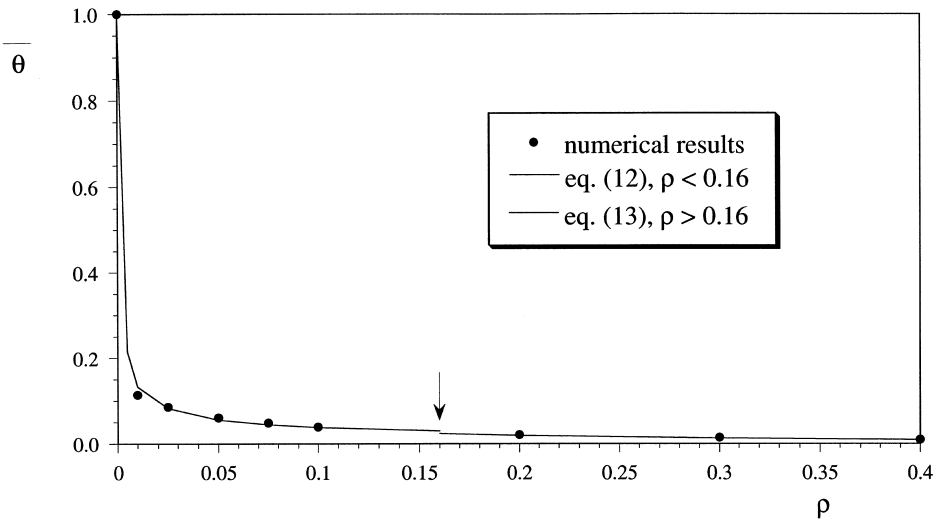

Fig. 10. Heat sink volume average nondimensional temperature vs. capsule density.

to λ, a result following from the normal random distribution of capsules within the domain. Eqs. (12) and (13) are empirical.

In Fig. 11 we present the results of the surface temperature gradient $|\nabla\theta|$ vs. the capsule density ρ. The curve fit equations in this case are

$$|\nabla\theta| = 1.668 \times 10^4 \lambda^{-1.24} \quad \text{for} \quad \rho < 0.16 \tag{14}$$

$$|\nabla\theta| = 1.162 \times 10^4 \lambda^{-2/3} \quad \text{for} \quad \rho > 0.16 \tag{15}$$

The dependence of $\bar{\theta}$ and $|\nabla\theta|$ on λ is no coincidence: the diffusion process inside the domain is strongly related to the average distance between capsules.

The distinct behavior observed in both graphs of Figs. 10 and 11, as ρ varies, is the consequence of an interesting phenomenon. As the capsule density increases, more and more sites inside the domain are occupied by encapsulated PCM, and therefore behave as isothermal nodes. Observe that with enough sites selected as capsules sites (high capsule density), one particular capsule site may be surrounded by other sites, also occupied by capsules. In this case, the surrounded site has no effect on the diffusion capability of the domain because it does not participate effectively in the diffusion process as the heat flux is not allowed to reach this site.

The same can be said of a regular site that happens to be surrounded by capsule sites. In both cases, the capsules isolate the interior site from the diffusion process. We can then recognize a change in the diffusion behavior as the capsule density increases. The diffusion process seems to switch from a *disperse*-type, when the capsules do not interfere much with each other, to a *concentrate*-type when the capsules are close enough to each other to compete for the available energy coming from the heated surface. In this case, as the capsule density increases further, the capsules near the heated surface of the domain build a shield depleting the interior of energy diffusing from the boundary. The capsules placed far from the heated surface of the domain, will participate in the diffusion process only after enough energy is given to the participating capsules, to melt all the solid PCM material within them. From this point on, the heat sink device loses in thermal performance as the layer with molten PCM will behave as a sensible heat barrier for isothermal cooling, and the heating process evolves in a time-dependent manner.

With Eqs. (14) and (15) in Eq. (9), one can obtain two equations for the effective conductivity k_{eff} of the heat sink during phase-change, namely

$$k_{\text{eff}} = 5.995 \times 10^{-5} U \lambda^{1.24} \quad \text{for} \quad \rho < 0.16 \tag{16}$$

$$k_{\text{eff}} = 8.606 \times 10^{-5} U \lambda^{2/3} \quad \text{for} \quad \rho > 0.16 \tag{17}$$

For a certain capsule density value and a known (measured) U value, the estimated effective diffusivity, from Eqs. (16) or (17), can be used with the macroscopic model, Eq. (5), to simulate the transient diffu-

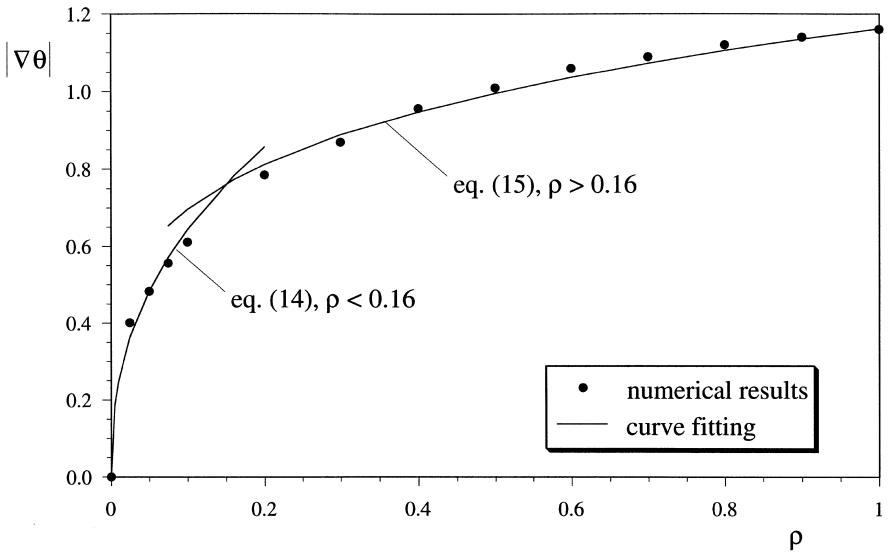

Figure 11

Fig. 11. Surface gradient of the volume average nondimensional temperature vs. capsule density.

sion process within the heat sink. Observe that the methodology for obtaining the effective thermal conductivity of the composite heat sink device is general and valid for any geometry, and not necessarily cubic.

5. Summary and conclusions

To improve the thermo-mechanical performance of solid-to-liquid PCM heat sinks, a new composite heat sink device (CHSD) design, based on a solid porous matrix filled with a transfer material embedding encapsulated PCM, is considered.

A simplified macroscopic model for the phase-change process within a CHSD, based on the volumetric average of the microscopic diffusion equations, is presented. Even though the complex internal geometry of the device precludes the direct calculation of effective thermal conductivity of the domain during the phase-change process, an alternate procedure is presented based on the overall heat transfer coefficient (measurable in the laboratory at steady-state) and the temperature gradient across the boundary of the device.

The effect of the encapsulated PCM density on the transient phase-change process is studied by considering the steady-state process, i.e., when the boundary temperature gradient can be calculated independently of the effective thermal conductivity of the device. Steady-state diffusion is then simulated numerically, considering a cubic CHSD heated isothermally from the bottom face, with all other faces being adiabatic. Capsules filled with PCM are simulated by setting the temperature at randomly selected sites within the domain equal to the saturating temperature of the PCM.

Results for various capsule density values are obtained, demonstrating the existence of two distinct diffusion processes. At low capsule density (less than 16%), the diffusion from the heated face to the capsules is mainly *disperse*, i.e., the capsules almost do not interfere with each other. In this case, the resulting effective thermal conductivity is expected to be high, decreasing with an increase in the encapsulated PCM density.

At high capsule density (greater than 16%), the diffusion is *concentrate*, i.e., the capsules do interfere with each other competing for the heat flux. For concentrate-type diffusion, the capsules placed near the heated face of the device form a shield absorbing the heat coming from the boundary. The capsules placed away from the heated face participate less effectively in the diffusion process due to having less access to the heat coming from the boundary.

The concentrate-type diffusion process is mainly between the heated face of the domain and an effective surface formed by the capsules located nearest to the heated boundary. In this case, the shape of the heat sink becomes less important, and the diffusion process becomes more unidimensional and primarily perpendicular to the heat sink surface. This configuration is less likely to yield isothermal cooling than the disperse-configuration, because the interior capsules will become effective phase-change players only after the PCM within the capsules of the shield layer melt, forming a sensible-heat liquid layer. When this happens, the heated surface will have to increase its temperature, to maintain the same level of heat flux absorbed by the heat sink.

References

[1] A. Bar-Cohen, Thermal management of electronic components with dielectric liquids, JSME Int. J 36 (Serie B) (1993) 21–34.
[2] M.B. Bowers, I. Mudawar, High heat flux boiling in low flow rate, low pressure drop mini-channel and micro-channel heat sinks, Int. J. Heat Mass Transfer 37 (1994) 321–332.
[3] J.L. Lage, A.K. Weinert, D.C. Price, R.M. Weber, Numerical study of a low permeability microporous heat sink for cooling phased-array radar systems, Int. J. Heat Mass Transfer 39 (1996) 3633–3647.
[4] B.V. Antohe, J.L. Lage, D.C. Price, R.M. Weber, Numerical characterization of micro heat exchangers using experimentally tested porous aluminum layers, Int. J. Heat Fluid Flow 17 (1996) 594–603.
[5] R.L. Webb, Principles of Enhanced Heat Transfer, Wiley, New York, 1994.
[6] K.W. Snyder, An investigation of using a phase-change material to improve the heat transfer in a small electronic module of an airborne radar application, in: Proceedings of the Int. Electronics Packaging Conference, San Diego, CA, vol. 1, 1991, pp. 276–303.
[7] J.P. O'Connor, R.W. Weber, Thermal management of electronic packages using solid-to-liquid phase change techniques, in: Proceedings of the 1997 Int. Systems Packaging Symposium, International Microelectronics and Packaging Society (IMAPS), 1997, pp. 72–80.
[8] K.A.R. Ismail, M.R.B. Trullenque, Finned rectangular cavities filled with PCM for thermal control of electronic equipments, in: J.S. Lee, S.H. Chung, K.Y. Kim (Eds.), Transport Phenomena in Thermal Engineering, vol. 1, Meckler, Westport–London, 1993, pp. 237–242.
[9] S. Whitaker, The Method of Volume Averaging, Kluwer Academic Publishers, Dordrecht, 1999.
[10] M. Kaviany, Principles of Heat Transfer in Porous Media, Springer–Verlag, New York, 1991, pp. 117–120.